Available online at www.sciencedirect.com
SCIENCE DIRECT®
Journal of Power Sources 119–121 (2003) 189–194
JOURNAL OF POWER SOURCES
www.elsevier.com/locate/jpowsour

Multiple-ion-doped lithium nickel oxides as cathode materials for lithium-ion batteries

G.X. Wang*, Steve Bewlay, Jane Yao, Y. Chen, Z.P. Guo, H.K. Liu, S.X. Dou

Battery Technology Research Program, Institute for Superconducting & Electronic Materials, University of Wollongong, Wollongong, NSW 2522, Australia

Abstract

Several multiple-ion-doped lithium nickel oxides with formula of $LiMn_xCo_yNi_{1-x-y}O_2$ were synthesized via solid-state reactions at high temperature. These phase-pure $LiMn_xCo_yNi_{1-x-y}O_2$ compounds have a layered hexagonal structure, and their electrochemical properties were systematically investigated. Typical cathodes can deliver a capacity in the range of 140–180 mAh/g with fairly stable cyclability. The kinetics of lithium insertion in these cathodes were characterized via ac impedance measurements. These newly developed compounds show great promises as cathode materials for future lithium-ion batteries with low cost and less toxicity.

Keywords: Lithium-ion battery; Cathode; Ion-doping; ac impedance

1. Introduction

Lithium-ion batteries are the state-of-the-art power sources for modern portable electronic devices such as laptop computers, cellular phones and camcorders. They have the highest energy density and longest cycle life among available rechargeable batteries. Large-scale lithium-ion batteries also have great potential for electric vehicles and stationary energy storage systems, and they are dominating the rechargeable battery market, replacing nickel–cadmium and nickel metal hydride batteries, due to their excellent performance. The electrochemical properties of cathode materials in lithium-ion batteries are very critical for the overall battery performance. The operation of lithium-ion batteries relies on the extraction and insertion of lithium ions in both cathode and anode hosts, however, the lithium-ion source is provided entirely by cathode materials. Three classes of materials, e.g. $LiCoO_2$, $LiNiO_2$ and $LiMn_2O_4$ compounds have been developed as cathode materials for lithium-ion batteries [1–5]. Among them, the structurally ordered $LiNiO_2$ compounds are difficult to synthesize and their cyclability is very poor [6–8]. $LiMn_2O_4$ spinels have low specific capacity and are structurally unstable for lithium-ion intercalation and de-intercalation [9–12]. Currently, $LiCoO_2$ cathode materials are widely used in commercial lithium-ion battery production. However, $LiCoO_2$ compounds are expensive, toxic, and therefore not environmentally benign. Also, the capacity of $LiCoO_2$ is limited to about 140 mAh/g. So, it is necessary to develop new cathode compounds for lithium-ion batteries, which are less expensive, non-toxic and have good electrochemical performance. The basic strategy is to prepare lithium nickel oxides base materials with stable structural and electrochemical properties. The structural integrity must be maintained, so that the electrochemical properties can be retained. Such new cathode materials must be inexpensive, therefore are crucial for making large-scale lithium-ion batteries for electric vehicles and stationary energy storage application in the future.

In this paper, a series of multiple-ion-doped lithium nickel oxides were synthesized. Phase-pure $LiMn_xCo_yNi_{1-x-y}O_2$ compounds with layered hexagonal structure were obtained. The structural and electrochemical properties of these cathode compounds were systematically investigated.

2. Experimental

Compounds were prepared by a special spray–dry technique. Reagents of Mn_2O_3 (Aldrich, 99.9%), Co_3O_4 (OMG, 99.9%), NiO (Aldrich, 99.9%), and Li_2CO_3 (Pacific Lithium Ltd., 99.9%) were mixed thoroughly in de-ionised water by using a planetary ball-milling machine. After ball-milling, a

* Corresponding author. Fax: +61-2-42215731.
E-mail address: gwang@uow.edu.au (G.X. Wang).

0378-7753/03/$ – see front matter © 2003 Elsevier Science B.V. All rights reserved.
doi:10.1016/S0378-7753(03)00177-0

homogeneous slurry was obtained. The slurry was then spray–dried using a laboratory-type mini spray drier. The spray dried precursor powders consist of spherical agglomerates, in which Li_2CO_3, Mn_2O_3, Co_3O_4 and NiO are uniformly distributed. The as-prepared precursors were loaded in an alumina crucible and then sintered in a tube furnace at a temperature range of 800–900 °C under oxygen gas flow. Three compounds $LiMn_{0.2}Co_{0.1}Ni_{0.7}O_2$, $LiMn_{0.2}Co_{0.25}Ni_{0.55}O_2$ and $LiMn_{0.2}Co_{0.3}Ni_{0.5}O_2$ were prepared in this investigation.

X-ray diffraction (XRD) was performed on $LiMn_xCo_yNi_{1-x-y}O_2$ powders using a Philips 1730 diffractometer with a Cu Kα radiation. For electrochemical testing, cathodes were made by dispersing 85% active material, 10% acetylene carbon black and 5% poly(vinylidene fluoride) in dimethyl phthlate solvent. The slurry was then coated on an Al foil. Teflon test cells were assembled in an argon-filled glove-box. Each cell contained a lithium foil as anode and 1 M $LiPF_6$ in a mixture of 50 vol.% ethylene carbonate (EC) and 50 vol.% dimethyl carbonate (DMC) as electrolyte. Cells were cycled between 3.0 and 4.5 V.

Cyclic volatammetry (CV) was carried out using a EG & G potentiostat (Model M362) at a scanning rate of 0.1 mV/s. The ac impedance measurements were also performed using an impedance analyzer (Model 6310, EG & G Princeton Applied Research). Before ac impedance measurements, the cell was pre-cycled between 3.0 and 4.5 V for five cycles to establish and stablise the solid electrolyte interface (SEI) between the electrolyte and electrodes. The cells were then potentiostatically conditioned to a potential and equilibrated for 2 h, then, ac impedance spectra were obtained by applying a sine wave of 5 mV amplitude over the frequency range of 100 kHz to 1 mHz.

3. Results and discussion

3.1. Physical and structural characterization

Fig. 1 shows the SEM image of $LiMn_{0.2}Co_{0.25}Ni_{0.55}O_2$ compound. Homogeneous crystals and crystal size distribution can be obtained by properly controlling the syntheses conditions. To determine the distribution of Mn, Co and Ni ions in $LiMn_xCo_yNi_{1-x-y}O_2$ compounds, EDS mapping was performed. The results of EDS mapping show a very uniform distribution of Mn, Co, Ni ions in the crystal structure, which can be attributed to the process of intensive ball-milling and subsequent slurry spray–drying. During ball-milling process, the raw materials containing Mn, Co, and Ni are mixed in a quasi-atomic level. The slurry spray–drying process forms the spherical agglomerates, which consist of multiple reactant phases such as Li_2CO_3, Mn_2O_3, Co_3O_4 and NiO. These reactant particles are closely contacted each other within the agglomerates. The spherical precursor agglomerates are shown in Fig. 2. When heating to high temperature, solid solutions of $LiMn_xCo_yNi_{1-x-y}O_2$ compounds are formed via solid-state reactions.

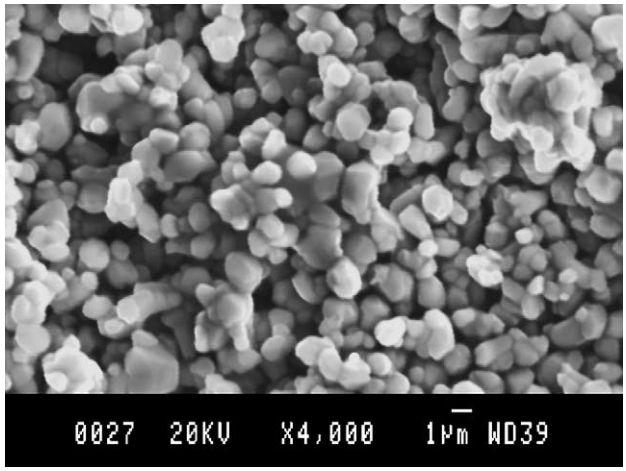

Fig. 1. SEM image of $LiMn_{0.2}Co_{0.25}Ni_{0.55}O_2$ compound.

The crystal structure of $LiMn_xCo_yNi_{1-x-y}O_2$ compounds was characterized by X-ray diffraction. Fig. 3 shows the X-ray diffraction patterns of three different $LiMn_xCo_yNi_{1-x-y}O_2$ compounds. Phase-pure solid-state solution with a hexagonal structure (*R*3*m*) was successfully obtained for different amount of Co, Mn and Ni. In this hexagonal structure, lithium and transition metal ions are ordered in alternate (1 1 1) planes between two oxygen planes along the "*C*"-axis. Li^+ and M^{3+} ions occupy 3a and 3b sites, respectively. Such a layered framework provides a two-dimensional interstitial site which allows for relatively facile extraction and insertion of lithium ions.

The *h k l* indices for hexagonal structure are labeled in Fig. 3. All diffraction lines are indexed to the hexagonal phase. No impurity phase was observed, which indicates that a solid-state solution can be formed in a wide range of Mn, Co and Ni contents for the $LiMn_xCo_yNi_{1-x-y}O_2$ system. Previously, there were many reports about binary transition metal $LiM_xM'O_2$ systems such as $LiCo_xNi_yO_2$, $LiMn_xNi_{1-x}O_2$, $LiAl_xNi_{1-x}O_2$, etc. Here, we report that the ternary

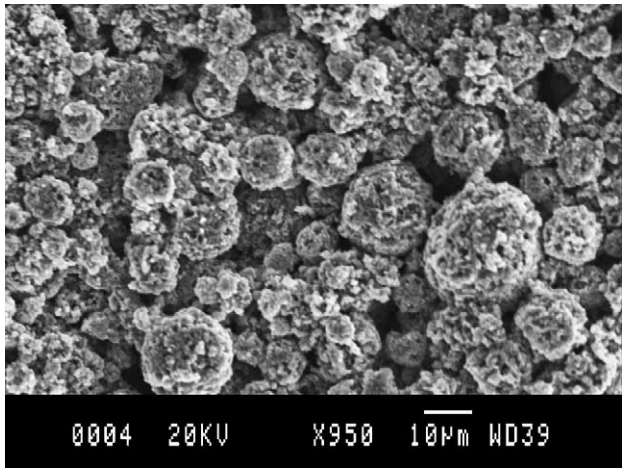

Fig. 2. SEM image of spherical spray–dried $LiMn_{0.2}Co_{0.25}Ni_{0.55}O_2$ precursors.

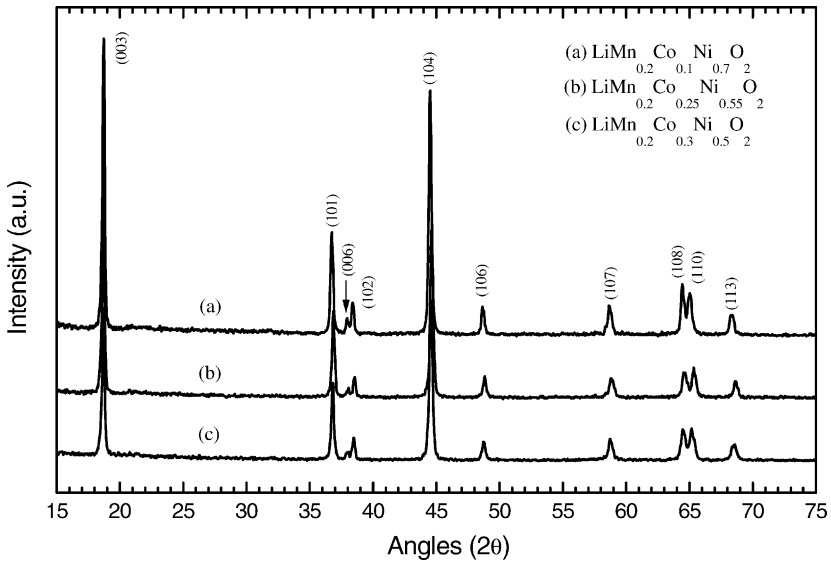

Fig. 3. X-ray diffraction patterns of $LiMn_xCo_yNi_{1-x-y}O_2$ compounds.

transition metal $LiM_xM_y'M_z''O_2$ system with pure phases can be successfully synthesized. Unit cell parameters for the hexagonal $LiMn_xCo_yNi_{1-x-y}O_2$ phase were determined. In comparison, the lattice parameters of $LiCoO_2$ and $LiNiO_2$ are also presented in Table 1. The $LiNiO_2$ has large lattice parameters "*a*" and "*c*" than those of $LiCoO_2$. With the mixing of Mn, Co and Ni ions in the 3b sites, the lattice parameters "*a*" and "*c*" $LiMn_xCo_yNi_{1-x-y}O_2$ compounds change with the variation of the composition. However, we did not identify the relationship between the compositions and lattice parameters. More systematic work requires to be done.

Table 1
The lattice parameters of $LiMn_xCo_yNi_{1-x-y}O_2$ compounds

Compounds	*a* (Å)	*c* (Å)
$LiMn_{0.2}Co_{0.1}Ni_{0.7}O_2$	2.862	14.153
$LiMn_{0.2}Co_{0.25}Ni_{0.55}O_2$	2.845	14.124
$LiMn_{0.2}Co_{0.3}Ni_{0.5}O_2$	2.858	14.140
$LiCoO_2$	2.819	14.066
$LiNiO_2$	2.882	14.194

3.2. Electrochemical testing of $LiMn_xCo_yNi_{1-x-y}O_2$ cathode materials

Cyclic voltammetry measurements were performed on the $LiMn_xCo_yNi_{1-x-y}O_2$ electrodes. Fig. 4 shows the cyclic

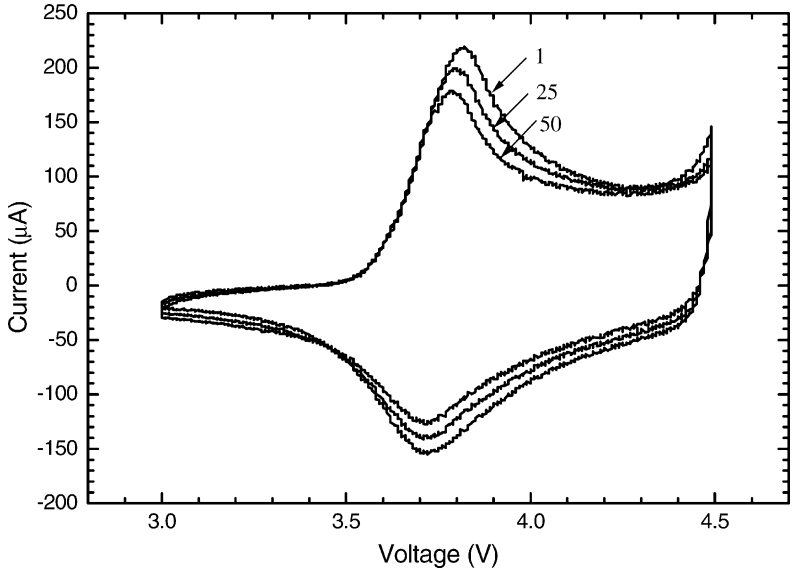

Fig. 4. Cyclic voltammograms of $LiMn_{0.2}Co_{0.25}Ni_{0.55}O_2$ compound. Scanning rate: 0.1 mV/s.

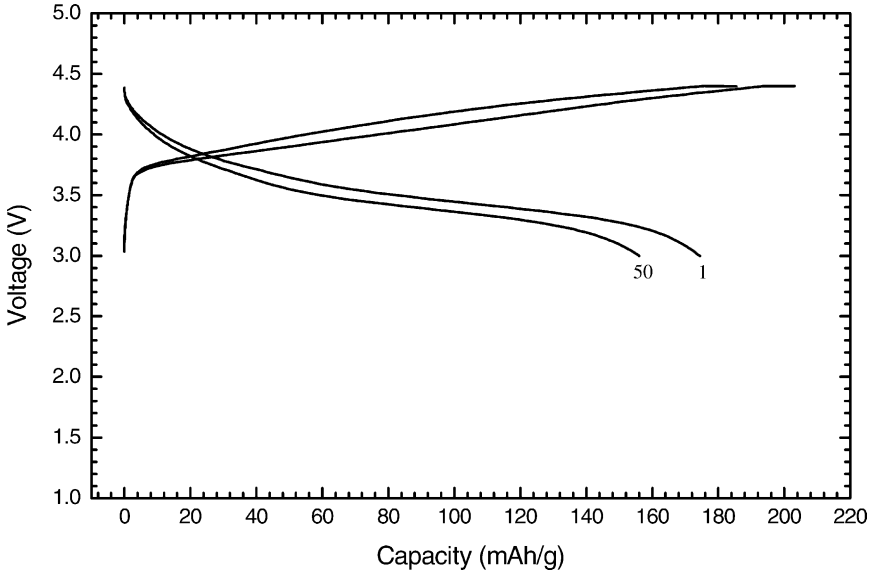

Fig. 5. The charge and discharge curves of $LiMn_{0.2}Co_{0.25}Ni_{0.55}O_2$ electrode.

voltammograms of $LiMn_{0.2}Co_{0.25}Ni_{0.55}O_2$ electrode. A pair of redox peaks was observed in the voltage range of 3.0–4.5 V, which corresponds to the lithium intercalation and lithium de-intercalation reactions. The reduction peaks are much broader than the oxidation peaks, but the reason is not clear. These CV curves are similar to those for $LiCoO_2$ and $LiNiO_2$ cathodes. In the subsequent scanning cycles, the intensity of the reduction peaks and oxidation peaks decreases, but without changes of their positions and shapes. The monoclinic $LiMnO_2$ and doped $LiM_xMn_{1-x}O_2$ compounds always experience a transformation to a cubic spinel phase [13,14], which usually demonstrates a split reduction peak and oxidation peak in the CV curve. Since there are 20% Mn presented in $LiMn_{0.2}Co_{0.25}Ni_{0.55}O_2$, it is not sure if $LiMn_{0.2}Co_{0.25}Ni_{0.55}O_2$ electrode is structurally stable when experiencing lithium extraction and insertion cycling. We did not observe any change of the redox peaks in the CV curves, which indirectly indicates that the $LiMn_{0.2}Co_{0.25}Ni_{0.55}O_2$ electrode is stable. Therefore, a transformation to the cubic spinel phase is unlikely to occur for $LiMn_xCo_yNi_{1-x-y}O_2$ compounds. Further confirmation requires performing in situ X-ray diffraction.

Constant-current charge/discharge cycling tests were carried out to determine specific capacity and cyclability. Fig. 5

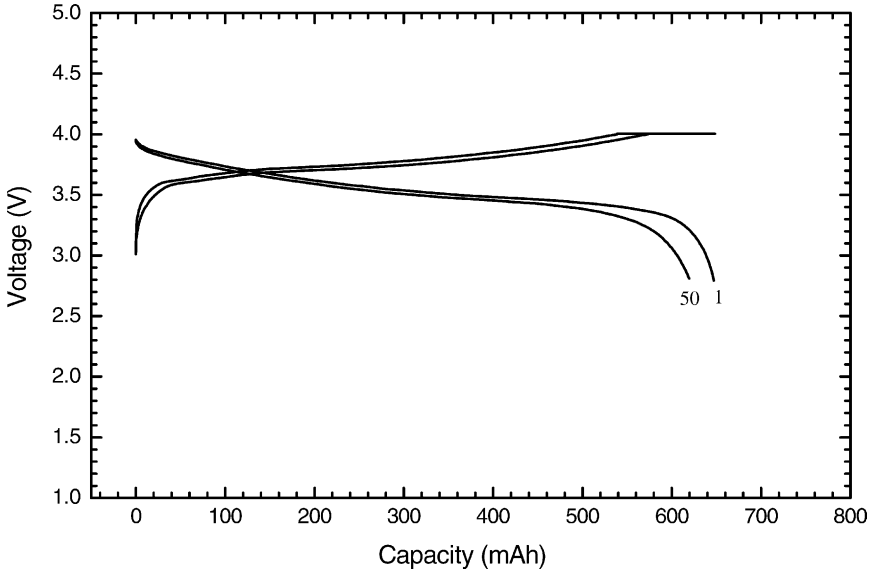

Fig. 6. The charge and discharge curves of a rectangular Li-ion battery using $LiMn_{0.2}Co_{0.25}Ni_{0.55}O_2$ as cathode and MCMB carbon as anode.

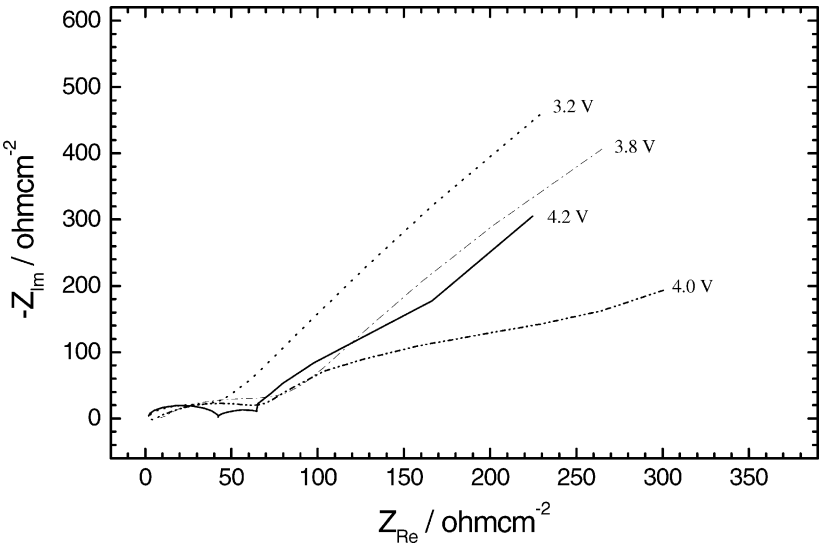

Fig. 7. The ac impedance spectra of $LiMn_{0.2}Co_{0.25}Ni_{0.55}O_2$ electrode.

shows the charge/discharge profiles of $LiMn_{0.2}Co_{0.25}Ni_{0.55}O_2$ electrode. In the first cycle, it has reached a specific charging capacity of 214 mAh/g and discharging capacity of 180 mAh/g. A capacity of 34 mAh/g was lost during the first cycle, which could be attributed to the formation of a passivation film on the surface of the electrode. The discharge capacity still retains 85% of the initial capacity after 50 cycles. The average discharge potential of $LiMn_xCo_yNi_{1-x-y}O_2$ electrode is about 3.5–3.6 V versus a lithium reference electrode, which is slightly lower than that of pure $LiCoO_2$ and $LiNiO_2$ electrodes. The order of operating voltage for Mn, Co and Ni oxides is approximately: CoO_2 ($3d^5/3d^6$) > NiO_2 ($3d^6/3d^7$) > MnO_2(II) ($3d^3/3d^4$). MnO_2(II) designated operating voltage at 3.0 V [15]. The participation of Mn in redox reaction could possibly influence the chemical potential of the electrode materials. Through adjusting the doping ions and their concentrations, the chemical potential of the cathode materials can be modified. Such work is currently underway in our laboratory.

The rectangular lithium-ion batteries were assembled using the as-synthesed $LiMn_{0.2}Co_{0.25}Ni_{0.55}O_2$ compound as cathode material and mesocarbon microbeads (MCMB) as anode material. Fig. 6 shows the charge and discharge curves. The average discharging voltage of the battery is about 3.5 V. When coupled with MCMB carbon anode, the cells demonstrated stable cyclability. This is a very promising result for their use as future cathode materials.

The electrochemical impedance spectra of $LiMn_{0.2}Co_{0.25}Ni_{0.55}O_2$ electrodes were measured at different charging states. The typical Nyquist plots are presented in Fig. 7. A semicircle was observed to center on the real axis at high frequencies range. In the low frequency range, a straight line at 45° to the real axis corresponds to the Warburg impedance. A second semicircle was observed at the highly charged state. A passivation layer formed on the surface of the electrode could be responsible for this second semicircle. The $LiMn_{0.2}Co_{0.25}Ni_{0.55}O_2$ electrode demonstrated a behavior similar to the $LiCoO_2$ and $LiNiO_2$ electrodes.

4. Conclusions

Ternary transition metal doped $LiMn_xCo_yNi_{1-x-y}O_2$ compounds were successfully prepared by solid-state reaction. These phase-pure compounds have a hexagonal layered structure. Cyclic voltammetry measurements show a pair of redox reaction peaks, similar to $LiCoO_2$ electrodes. The $LiMn_xCo_yNi_{1-x-y}O_2$ electrode exhibited a lower discharge potential than $LiCoO_2$, but they demonstrated stable cyclability in lithium-ion batteries. $LiMn_xCo_yNi_{1-x-y}O_2$ compounds have great potential to be used as cathode materials for lithium-ion batteries with low cost and low toxicity.

Acknowledgements

The financial support from Australia Research Council (ARC) is greatly acknowledged.

References

[1] K. Mizushima, P.C. Jones, P.J. Wiseman, J.B. Goodenough, Mater. Res. Bull. 17 (1980) 783.
[2] T. Ohzuku, A. Ueda, J. Electrochem. Soc. 141 (1994) 2972.
[3] C. Delmas, Mater. Sci. Eng. B 3 (1989) 97.
[4] T. Ohzuku, A. Ueda, M. Nagayama, J. Electrochem. Soc. 140 (1993) 1862.

[5] J.R. Dahn, U. Von Sacken, C.A. Michal, Solid State Ionics 44 (1990) 87.
[6] J.N. Reimers, W. Li, J.R. Dahn, Phys. Rev. B 47 (1993) 8486.
[7] A. Rougier, P. Gravereau, C. Delmas, J. Electrochem. Soc. 143 (1996) 1168.
[8] R.V. Moshtev, P. Zlatilova, V. Manev, Atsushi Sato, J. Power Sources 54 (1995) 329–333.
[9] M.M. Thackeray, A. de Kock, M.H. Rossouw, D.C. Liles, D. Hoge, R. Bittchn, J. Electrochem. Soc. 139 (1992) 363.
[10] K.M. Colbow, J.R. Dahn, R.R. Haering, J. Power Sources 26 (1989) 397.
[11] G.X. Wang, D.H. Bradhurst, H.K. Liu, S.X. Dou, Solid State Ionics 120 (1999) 95–101.
[12] G.X. Wang, S. Zhong, D.H. Bradhurst, S.X. Dou, H.K. Liu, Solid State Ionics 116 (1999) 271–277.
[13] A. Robert Armstrong, P.G. Bruce, Nature 381 (1996) 499.
[14] I.M. Kotschau, J.R. Dahn, J. Electrochem. Soc. 145 (1998) 2672.
[15] A. Ueda, T. Ohzuku, J. Electrochem. Soc. 141 (1994) 2010.